



# Instability of subcooled boiling film on a vertical wall

B.Y. Rubinstein<sup>a,\*</sup>, S.G. Bankoff<sup>b</sup>, S.H. Davis<sup>a</sup>

<sup>a</sup> Department of Engineering Sciences and Applied Mathematics, Northwestern University, 2145 Sheridan Road, Evanston, IL 60208-3125, USA

<sup>b</sup> Department of Chemical Engineering, Northwestern University, 2145 Sheridan Road, Evanston, IL 60208-3125, USA

Received 7 September 2001; received in revised form 25 May 2002

## Abstract

Consider a vertical plate with a leading edge. The temperature of the plate is above the spontaneous nucleation temperature, so that vapor completely covers the plate. Two-dimensional quasi-parallel theory is used to examine the stability of the two-phase system. Numerical calculations show that the main parameter determining the thickness of the vapor film and its stability is the difference between the temperature of the heated vertical plate and the saturation temperature of the liquid. As the thickness of the vapor film is made smaller, the nose of the neutral curve approaches that of the corresponding one-phase liquid. The overall temperature difference between the plate and liquid bulk does not strongly influence stability properties.

© 2002 Elsevier Science Ltd. All rights reserved.

## 1. Introduction

Film boiling of a volatile liquid from a hot solid surface occurs when the surface temperature is above a critical temperature, known as the minimum film-boiling temperature (MFBT). Above this point contacts between the liquid and solid are only momentary. At solid surface temperatures below this point a rapid transition can occur to nucleate boiling, with production of numerous vapor bubbles. Under vigorous surface boundary-layer agitation, the average heat transfer coefficient increases strongly, and quenching of the hot surface takes place, as in metal heat treating. The reverse process, in which nucleate boiling rapidly transits to film boiling, occurs at a critical heat flux, which constitutes a practical operating limit for boilers and nuclear reactors. Because of the obvious safety implications, these transitions have been widely studied. Nucleate boiling is a highly chaotic process, dependent on the irregular dis-

position and nature of nucleation sites. Hence an acceptable theory, devoid of empirical data, has not been achieved. The reverse process of film boiling–nucleate boiling transition is more tractable, since close to MFBT, the vapor layer is usually laminar and smooth. Hydrodynamic stability (Rayleigh–Taylor) models [1] have therefore been formulated for horizontal surfaces, but often have been applied to situations where the theory should not hold, as in boiling on vertical walls, cylinders and spheres. With the application of empirical correction factors, however, reasonably good prediction tools have been obtained.

At high liquid subcoolings, the vapor layer tends to be quite thin, and will quickly break up unless the solid surface temperature is quite high. These circumstances lead to very large heat transfer rates, which are highly desirable for some applications. Another form of instability, known as heterogeneous spontaneous nucleation, then may become important. This refers to vapor-free heterogeneous nucleation, called by Fauske spontaneous nucleation [2,3], and studied experimentally by Waldram et al. [4]. Its counterpart, homogeneous nucleation, refers to spontaneous formation of critical-size vapor embryos through random thermal motion (Brownian motion) of the liquid molecules in the absence of a second phase. However, as pointed out by Skripov [5],

\* Corresponding author. Present address: Institute of Theoretical Dynamics, University of California—Davis, One Shields Avenue, Davis, CA 95616, USA. Tel.: +1-530-752-0938; fax: +1-530-752-7297.

E-mail address: [boris@itd.ucdavis.edu](mailto:boris@itd.ucdavis.edu) (B.Y. Rubinstein).

### Nomenclature

$A$	relative superheat, $A = (T_0 - T_s)/\Delta T$	$w$	velocity component normal to the wall
$a$	scaled wave number of perturbation	$x$	coordinate measuring distance along the wall
$d$	length scale	$z$	coordinate measuring distance normal to the wall
$E$	evaporation number, $E = k_l \Delta T / v_l \rho_{0l} L$	<i>Greek symbols</i>	
$G$	scaled gravity, $G = gd^3 / v_l^2$	$\alpha$	thermal expansion coefficient
$g$	acceleration of gravity	$\epsilon$	small amplitude of linear perturbation, $\epsilon = w/u$
$Gr$	Grashof number	$\kappa$	thermal diffusivity
$h$	position of the interface	$\mu$	dynamic viscosity
$\mathbf{I}$	unit tensor of the second rank	$\nu$	kinematic viscosity
$J$	mass flux	$\rho_0$	density
$k$	thermal conductivity	$\sigma$	surface tension
$L$	latent heat of vaporization	$\Psi$	stream function
$\mathbf{n}$	unit vector normal to the interface	$\omega$	scaled frequency of perturbation
$p$	pressure	$\nabla$	two-dimensional differentiation operator, $\nabla = \{\partial/\partial x, \partial/\partial z\}$
$Pr$	Prandtl number	<i>Subscripts</i>	
$Re$	Reynolds number	$c$	critical value
$S$	surface tension	$d$	dimensional value
$T$	temperature	$i$	interface
$T_\infty$	liquid temperature far from the wall	$l$	liquid
$T_L$	liquid temperature at finite very large distance from the wall	$v$	vapor
$T_s$	saturation temperature	$x$	derivative with respect to $x$
$T_0$	wall temperature	$z$	derivative with respect to $z$
$\Delta T$	overall temperature difference	$0$	basic flow
$t$	time	$1$	perturbation
$\mathbf{t}$	unit vector tangential to the interface		
$u$	velocity component parallel to the wall		
$V$	velocity scale, $V = g\alpha_l \Delta T / v_l d^2$		

the critical temperature may be substantially reduced if a second (unwetted) phase is present. An explosive local transition can then take place close to a heated wall. The subject has been thoroughly studied by Sakurai, Shiotsu and associates (see [6] and references therein) in a series of papers, covering a range of system pressures, liquids, solids, liquid temperature and flow. Heterogeneous spontaneous nucleation heat transfer is still not well understood, and requires empirical data as input, particularly in view of its highly turbulent nature.

Hydrodynamic stability theory can be quite useful in analyzing the transitions in film boiling on a heated vertical plate with a leading edge at which a boundary layer begins, develops with distance, and at some point undergoes a transition to turbulence. It is the object of the laminar analysis to determine the position at which there is a transition to a higher heat transfer occurs; this is the instability point, which here will be studied for two-dimensional quasi-parallel disturbances. The instability point translates into a position above the leading edge where disturbances begin to grow.

Unfortunately, there seem to be no data with which to compare our predictions. This work can therefore serve as a guide for such experiments.

## 2. Formulation of the model

Consider a semi-infinite vertical plate with a leading edge at  $x = 0$  as shown in Fig. 1. The plate is heated to uniform temperature  $T_0$  above the saturation temperature  $T_s$  of the adjacent liquid which at large distances from the plate is cooled to temperature  $T_\infty$ ,  $T_\infty < T_s$ . As a result of heating, and for  $T_0$  large enough, a vapor film is formed, separating the plate from the remaining liquid as shown.

The fluids are governed by the Boussinesq equations in each phase

$$\rho_0 \left( \frac{\partial \mathbf{v}}{\partial t} + \mathbf{v} \cdot \nabla \mathbf{v} \right) = -\nabla p^* + \mu \nabla^2 \mathbf{v} + \rho_0 \alpha g (T - T_L) \mathbf{e}_x, \quad (1)$$

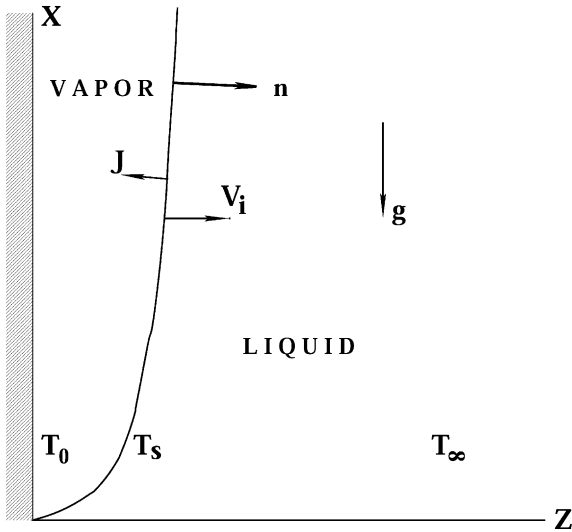


Fig. 1. Sketch of the model system.

$$\nabla \cdot \mathbf{v} = 0, \tag{2}$$

$$\frac{\partial T}{\partial t} + \mathbf{v} \cdot \nabla T = \kappa \nabla^2 T, \tag{3}$$

where the radiation heating is ignored. Subscripts v and l will label variables in the two phases. Here  $\mathbf{v} = \{u, w\}$  is the velocity,  $p^*$  is the reduced pressure,  $T$  is the temperature,  $\rho_0$ ,  $\mu$ ,  $\kappa$  and  $\alpha$  are the density, viscosity, thermal diffusivity, and thermal expansion coefficient of the fluid, respectively,  $\mathbf{e}_x = \{1, 0\}$  and  $g$  is the magnitude of the acceleration of gravity.

On the solid plate at  $z = 0, x \geq 0$

$$T_v = T_0, \tag{4}$$

and

$$\mathbf{v}_v = \mathbf{0}. \tag{5}$$

Far from the plate at  $z = l_*$

$$T_l = T_L \tag{6}$$

and a non-zero velocity is allowed in order to mimic the infinite domain case.

$$\mathbf{v}_l = \mathbf{v}_L = \text{const.} \tag{7}$$

According to Burelbach et al. [9] on the interface  $z = h(x, t)$ , the mass flux  $J$  through the interface from the liquid is given by

$$J = \rho_{0l}(\mathbf{v}_l - \mathbf{v}_i) \cdot \mathbf{n}, \tag{8}$$

which equals the flux from the vapor side

$$J = \rho_{0v}(\mathbf{v}_v - \mathbf{v}_i) \cdot \mathbf{n}, \tag{9}$$

where  $\mathbf{v}_i$  is the interface velocity and  $\mathbf{n}$  is the unit normal vector pointing out of the vapor. The normal-stress condition is

$$J(\mathbf{v}_v - \mathbf{v}_i) \cdot \mathbf{n} - (\mathbf{T}_v - \mathbf{T}_l) \cdot \mathbf{n} \cdot \mathbf{n} + \sigma \nabla \cdot \mathbf{n} = 0, \tag{10}$$

where  $\sigma$  is the constant surface tension and the stress tensor is given by

$$\mathbf{T} = -p\mathbf{I} + 2\mu\mathbf{D}, \quad \mathbf{D} = \frac{1}{2}[\nabla\mathbf{v} + (\nabla\mathbf{v})^T], \tag{11}$$

where  $p$  is the pressure,  $\mathbf{I}$  is unit tensor. The shear-stress condition reads

$$J(\mathbf{v}_v - \mathbf{v}_i) \cdot \mathbf{t} - (\mathbf{T}_v - \mathbf{T}_l) \cdot \mathbf{n} \cdot \mathbf{t} = 0. \tag{12}$$

There is the no-slip condition

$$\mathbf{v}_v \cdot \mathbf{t} = \mathbf{v}_l \cdot \mathbf{t}, \tag{13}$$

where  $\mathbf{t}$  is the unit tangential vector,

$$\mathbf{n} = \{-h_x, 1\} / \sqrt{1 + h_x^2}, \quad \mathbf{t} = \{1, h_x\} / \sqrt{1 + h_x^2}. \tag{14}$$

The energy balance at the interface takes the form:

$$J\{L + 1/2[(\mathbf{v}_v - \mathbf{v}_i) \cdot \mathbf{n}]^2 - 1/2[(\mathbf{v}_l - \mathbf{v}_i) \cdot \mathbf{n}]^2\} + k_l \nabla T_l \cdot \mathbf{n} - k_v \nabla T_v \cdot \mathbf{n} + 2\mu_l(\mathbf{D}_l \cdot \mathbf{n}) \cdot (\mathbf{v}_l - \mathbf{v}_i) - 2\mu_v(\mathbf{D}_v \cdot \mathbf{n}) \cdot (\mathbf{v}_v - \mathbf{v}_i) = 0, \tag{15}$$

where  $L$  is the latent heat of vaporization, and  $k$  denotes the thermal conductivity. Finally, one needs a relation that defines the interface temperature  $T_i$ ; here, we shall assume local thermodynamic equilibrium, which gives that

$$T_i = T_s. \tag{16}$$

### 3. Scalings

Simplification of the system (1)–(16) will be sought appropriate for the situation where all the heat arriving at the interface is available for phase change. Let  $d$  and  $V$  be scalings for the length and the velocity, both of which will be defined shortly. Define the superheat  $\Delta T$  across the layer:

$$\Delta T = T_0 - T_L, \tag{17}$$

and the non-dimensional temperature  $\hat{T}$  as

$$\hat{T} = \frac{T - T_L}{\Delta T}, \tag{18}$$

so that at the heated plate

$$\hat{T}_v = 1 \quad \text{at } \hat{z} = 0 \tag{19}$$

and far from the plate

$$\hat{T}_l = 0 \quad \text{at } \hat{z} = 1 \equiv l_*/d.$$

The bulk equations (1)–(3) are scaled as

$$\frac{\partial \hat{\mathbf{v}}_1}{\partial t} + \hat{\mathbf{v}}_1 \cdot \nabla \hat{\mathbf{v}}_1 = -\nabla \hat{p}_1 + \frac{1}{Re} \nabla^2 \hat{\mathbf{v}}_1 + \frac{Gr}{Re^2} \hat{T}_1 \mathbf{e}_x, \quad (20)$$

$$\frac{\partial \hat{\mathbf{v}}_v}{\partial t} + \hat{\mathbf{v}}_v \cdot \nabla \hat{\mathbf{v}}_v = -\frac{1}{\rho} \nabla \hat{p}_v + \frac{v}{Re} \nabla^2 \hat{\mathbf{v}}_v + \alpha \frac{Gr}{Re^2} \hat{T}_v \mathbf{e}_x, \quad (21)$$

$$\frac{\partial \hat{T}_1}{\partial t} + \hat{\mathbf{v}}_1 \cdot \nabla \hat{T}_1 = \frac{1}{Pr_1 Re} \nabla^2 \hat{T}_1, \quad (22)$$

$$\frac{\partial \hat{T}_v}{\partial t} + \hat{\mathbf{v}}_v \cdot \nabla \hat{T}_v = \frac{v}{Pr_v Re} \nabla^2 \hat{T}_v, \quad (23)$$

where  $Pr = \nu/\kappa$  denotes the Prandtl number, distinct for the vapor and liquid phase. At the interface at  $\hat{z} = \hat{h}(\hat{x}, \hat{t})$ , there are the mass-flux balances (8) and (9):

$$\begin{aligned} \frac{E\hat{J}}{Re} &= (\hat{\mathbf{v}}_1 - \hat{\mathbf{v}}_i) \cdot \mathbf{n}, \\ \frac{E\hat{J}}{Re} &= \rho(\hat{\mathbf{v}}_v - \hat{\mathbf{v}}_i) \cdot \mathbf{n}, \end{aligned} \quad (24)$$

the normal-stress condition:

$$\begin{aligned} \frac{E^2 \hat{J}^2}{Re^2} (1 - \rho^{-1}) + \hat{p}_1 - \hat{p}_v - \frac{2}{Re} (\hat{\mathbf{D}}_1 - \mu \hat{\mathbf{D}}_v) \cdot \mathbf{n} \cdot \mathbf{n} \\ = -\frac{S}{Re^2} \nabla \cdot \mathbf{n}, \end{aligned} \quad (25)$$

the shear-stress condition:

$$(\hat{\mathbf{D}}_1 - \mu \hat{\mathbf{D}}_v) \cdot \mathbf{n} \cdot \mathbf{t} = 0, \quad (26)$$

and the simplified energy balance under condition that  $l \gg 1$

$$\hat{J} + (\nabla \hat{T}_1 - k \nabla \hat{T}_v) \cdot \mathbf{n} = 0. \quad (27)$$

Here the kinetic energy and heat generation terms have been dropped in favor of the latent-heat release. There is the no-slip condition

$$(\hat{\mathbf{v}}_1 - \hat{\mathbf{v}}_v) \cdot \mathbf{t} = 0 \quad (28)$$

and the scaled version of the temperature difference across the vapor layer,

$$A = \frac{T_0 - T_s}{\Delta T},$$

which determines the vapor-layer thickness. Other parameters are ratios of the material constants

$$\begin{aligned} \rho &= \frac{\rho_{0v}}{\rho_{0l}}, \quad \mu = \frac{\mu_v}{\mu_l}, \quad v = \frac{\mu}{\rho}, \quad \kappa = \frac{\kappa_v}{\kappa_l}, \\ \alpha &= \frac{\alpha_v}{\alpha_l}, \quad k = \frac{k_v}{k_l}, \end{aligned}$$

the surface tension

$$S = d\rho_{0l}\sigma_0/\mu_1^2,$$

the evaporation number

$$E = k_1 \Delta T / v_1 \rho_{0l} L,$$

gravity

$$G = gd^3/v_1^2,$$

the Reynolds number

$$Re = dV/v_1,$$

and the Grashof number

$$Gr = g\alpha_l \Delta T d^3 / v_1^2.$$

On the one hand one may note that the evaporation number  $E$ , which is applicable to problems describing two different phases, and the Grashof number  $Gr$  which is usually used in single-phase problems, both depend on the temperature difference  $\Delta T$ . We shall select one of them to represent the influence of the controllable parameter  $\Delta T$ .

On the other hand there is a relation between  $Gr$  and  $Re$  which determines the relative magnitudes of terms in the rescaled Navier–Stokes equations (20) and (21). As soon as this relation is established we have only one parameter controlling the problem. We use the typical velocity scaling for the stability of one-phase flows (see [7,8] and references therein)

$$V = \frac{g\alpha_l \Delta T}{v_1} d^2, \quad (29)$$

corresponding to  $Gr = Re$ . The length scale  $d$  remains arbitrary, but the neutral stability results are independent of it, as it shown below in Section 6. In what follows we drop carats in the scaled variables.

#### 4. Basic-flow equations

The basic states corresponds to steady flow with a vapor layer and a boundary layer in the region originating at the leading edge and thickening upward. Since the buoyancy is the main driving force in the problem, the buoyancy term in Eqs. (20) and (21) must be retained.

The set of steady basic-flow equation reads

$$\mathbf{v}_1 \cdot \nabla \mathbf{v}_1 = \frac{1}{Re} \nabla^2 \mathbf{v}_1 + \frac{1}{Re} T_1 \mathbf{e}_x, \quad (30)$$

$$\mathbf{v}_1 \cdot \nabla T_1 = \frac{1}{Pr_1 Re} \nabla^2 T_1, \quad (31)$$

$$\mathbf{v}_v \cdot \nabla \mathbf{v}_v = \frac{v}{Re} \nabla^2 \mathbf{v}_v + \frac{\alpha}{Re} T_v \mathbf{e}_x, \quad (32)$$

$$\mathbf{v}_v \cdot \nabla T_v = \frac{v}{Pr_v Re} \nabla^2 T_v, \quad (33)$$

where we assume that the pressure gradient is negligible. The first two equations in component form are as follows:

$$u_1 u_{1x} + w_1 u_{1z} = \frac{1}{Re} (u_{1xx} + u_{1zz}) + \frac{1}{Re} T_1, \quad (34)$$

$$u_1 w_{1x} + w_1 w_{1z} = \frac{1}{Re} (w_{1xx} + w_{1zz}), \quad (35)$$

$$u_1 T_{1x} + w_1 T_{1z} = \frac{1}{Pr_1 Re} (T_{1xx} + T_{1zz}). \quad (36)$$

The usual boundary-layer approximation consists of introducing different scales for  $x$  and  $z$  derivatives, as well as for  $u$  and  $w$ , such as,

$$\partial/\partial x \sim 1, \quad \partial/\partial z \sim \epsilon^{-1}, \quad u \sim 1, \quad w \sim \epsilon.$$

The left hand side (l.h.s.) of the Eq. (34) should be of unit order, and so the leading term in the Laplacian,  $u_{zz}/Re$ , and the buoyancy term should be of the same order. This implies that  $Re \sim \epsilon^{-2}$  and  $T \sim \epsilon^{-2}$ . Then the l.h.s. of the temperature Eq. (36) is of order of  $\epsilon^{-2}$ , as is the leading term,  $T_{zz}/(Pr_1 Re)$ , in the r.h.s. Consider now the second Eq. (35); its l.h.s. is of order  $\epsilon$  as is  $w_{zz}/Re$  in r.h.s. So the original basic-flow equations reduce to the following set, in which  $Re$  and  $T$  are rescaled by  $\epsilon^{-2}$ . Similar considerations are applied to the vapor-phase equations to produce the following:

$$u_1 u_{1x} + w_1 u_{1z} = \frac{1}{Re} u_{1zz} + \frac{1}{Re} T_1, \quad (37)$$

$$u_1 T_{1x} + w_1 T_{1z} = \frac{1}{Pr_1 Re} T_{1zz}, \quad (38)$$

$$u_v u_{vx} + w_v u_{vz} = \frac{v}{Re} u_{vzz} + \frac{\alpha}{Re} T_v, \quad (39)$$

$$u_v T_{vx} + w_v T_{vz} = \frac{v}{Pr_v Re} T_{vzz}. \quad (40)$$

Since the stationary interface will have small slope, the surface tension is taken to be negligible, and so the approximate boundary conditions become

$$\frac{EJ}{Re} = -u_1 h_x + w_1, \quad (41)$$

$$\frac{EJ}{Re} = \rho(-u_v h_x + w_v), \quad (42)$$

$$u_z = \mu u_{vz}, \quad (43)$$

$$u_1 = u_v, \quad (44)$$

$$J + T_z - kT_{vz} = 0. \quad (45)$$

It should be noted here that if we want to retain mass flux  $J$  in (41) and (42) we are required to have  $J \sim \epsilon$ . Thus, the mass flux in (45) is negligible compared the other terms and must be omitted. We seek a similarity solution (for zero surface tension). Stream functions  $\Psi(x, z)$  are introduced through the relations:

$$u = \Psi_z, \quad w = -\Psi_x,$$

as well as two sets of similarity functions

$$\Psi_1(x, z) = \left(\frac{x}{Re}\right)^{3/4} f_1(\eta),$$

$$\Psi_v(x, z) = v \left(\frac{x}{Re}\right)^{3/4} f_v(\eta),$$

$$T_1(x, z) = g_1(\eta), \quad T_v(x, z) = g_v(\eta),$$

with similarity variable

$$\eta = Re^{1/4} z x^{-1/4}.$$

The equations determining the stream functions and temperature profiles read

$$f_1''' + \frac{3}{4} f_1'' f_1 - \frac{1}{2} f_1'^2 + g_1 = 0, \quad (46)$$

$$g_1'' + \frac{3}{4} Pr_1 f_1 g_1' = 0, \quad (47)$$

$$f_v''' + \frac{3}{4} f_v'' f_v - \frac{1}{2} f_v'^2 + \frac{\alpha}{v^2} g_v = 0, \quad (48)$$

$$g_v'' + \frac{3}{4} Pr_v f_v g_v' = 0. \quad (49)$$

The boundary conditions are

$$f_v(0) = f_v'(0) = 0, \quad g_v(0) = 1, \quad (50)$$

$$f_1'(\infty) = 0, \quad g_1(\infty) = 0, \quad (51)$$

$$g_1(\bar{\eta}) = g_v(\bar{\eta}) = 1 - A, \quad g_1'(\bar{\eta}) = \kappa g_v'(\bar{\eta}), \quad (52)$$

$$f_1(\bar{\eta}) = \mu f_v(\bar{\eta}), \quad f_1'(\bar{\eta}) = v f_v'(\bar{\eta}), \quad (53)$$

$$f_1''(\bar{\eta}) = \mu v f_v''(\bar{\eta}). \quad (54)$$

### 5. Basic-flow solution

Consider water and ethanol as typical liquids for the numerical calculations. Their material properties are presented in Table 1.

It is instructive first to calculate the *one-phase* basic state, which corresponds to solution of Eqs. (46) and (47) with the boundary conditions (50) and (51) with subscripts dropped. We find the basic-flow solutions for air ( $Pr = 0.73$ ), ethanol ( $Pr = 5.68$ ), and water ( $Pr = 1.76$ ); the temperature and velocity profiles for water are shown in Fig. 2(a). Notice that the velocity profiles are inflectional, and the temperature profiles possess horizontal gradients, both suggestive of possible instabilities. These results agree with the calculations performed in [7]. The basic-flow profiles for ethanol do not differ qualitatively from these and are not shown here.

The basic-flow solution for the *two-phase* model is found as the solution of system (46)–(54); the quantities to be determined are  $f_v''(0)$  and  $g_v'(0)$ . The conditions (51) far from the solid wall are satisfied by minimizing a value of  $f_1'^2(l) + f_1''^2(l) + g_1^2(l)$  for  $l \gg 1$ .

Table 1  
Thermophysical material properties of liquids at 1 atm

	Water	Ethanol
$T_s$ (K)	373	352
$\rho_{0l}$ (g/m <sup>3</sup> )	$9.6 \times 10^5$	$7.9 \times 10^5$
$\rho_{0v}$ (g/m <sup>3</sup> )	$6.0 \times 10^2$	$1.6 \times 10^3$
$\nu_l$ (m <sup>2</sup> /s)	$3.0 \times 10^{-7}$	$5.0 \times 10^{-7}$
$\nu_v$ (m <sup>2</sup> /s)	$2.1 \times 10^{-5}$	$6.2 \times 10^{-5}$
$k_l$ (J/m s °C)	$6.8 \times 10^{-1}$	$1.7 \times 10^{-1}$
$k_v$ (J/m s °C)	$2.4 \times 10^{-2}$	$1.7 \times 10^{-2}$
$\kappa_l$ (m <sup>2</sup> /s)	$1.7 \times 10^{-7}$	$8.8 \times 10^{-8}$
$\kappa_v$ (m <sup>2</sup> /s)	$2.0 \times 10^{-5}$	$7.0 \times 10^{-6}$
$\alpha_l$ (1/°C)	$6.0 \times 10^{-4}$	$8.6 \times 10^{-4}$
$\alpha_v$ (1/°C)	$6.0 \times 10^{-3}$	$3.6 \times 10^{-3}$
$L$ (J/g)	$2.3 \times 10^3$	$8.8 \times 10^2$
$\sigma_0$ (N/m °C)	$5.9 \times 10^{-4}$	$2.0 \times 10^{-4}$

The basic solutions for water and steam are presented in Fig. 2(b)–(d) for different values of the relative superheat  $A$ . Again, the velocity profiles are inflectional, and the temperature profiles possess horizontal gradients. This means that we may expect the two types of instabilities which were detected for one-phase problem in [7]. We see that the parameter  $A$  controls the relative width of the vapor film on the wall, with smaller  $A$  corresponding to the thinner vapor film.

**6. Linear stability problem**

In deriving the linear disturbance equations we assume that the flow is quasi-parallel, so that all  $x$  deriv-

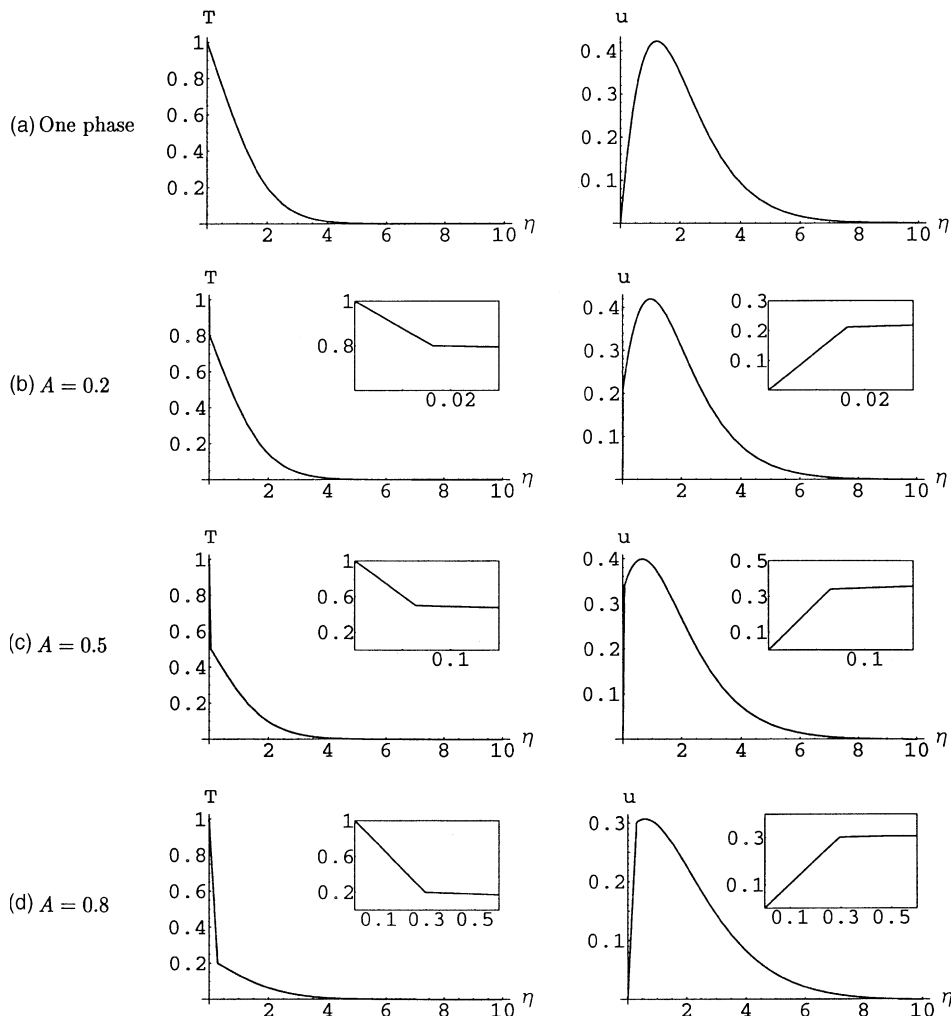


Fig. 2. The profiles of temperature  $T$  (left) and tangential velocity component  $u$  (right) as similarity solutions of basic-state problem for water (a) the one-phase problem, and the two-phase problem for (b)  $A = 0.2$ , (c)  $A = 0.5$ , (d)  $A = 0.8$ . The insets show enlarged profiles in the vapor–liquid interface region.

atives of the basic-flow quantities are set to zero. In this case all first-order disturbances  $Q_1$  can be written in the form

$$Q_1(x, z, t) = Q_1(z)e^{i(\hat{a}x - \hat{\omega}t)}.$$

In the liquid

$$u_{1lx} + w_{1l}u_{0lz} + u_{0l}u_{1lx} = -p_{1lx} + \frac{1}{Re}(u_{1lxx} + u_{1lzz}) + \frac{1}{Re}T_{1l}, \tag{55}$$

$$w_{1lx} + u_{0l}w_{1lx} = -p_{1lz} + \frac{1}{Re}(w_{1lxx} + w_{1lzz}), \tag{56}$$

$$T_{1lx} + w_{1l}T_{0lz} + u_{0l}T_{1lx} = \frac{1}{Pr_l Re}(T_{1lxx} + T_{1lzz}). \tag{57}$$

Similar equations could be written for the vapor phase. In terms of the normal modes we have

$$-i\hat{\omega}D\Psi_{1l} - i\hat{a}\Psi_{1l}\Psi_{0lzz} + i\hat{a}\Psi_{0lz}D\Psi_{1l} = -i\hat{a}p_{1l} + \frac{1}{Re}(D^2 - \hat{a}^2)D\Psi_{1l} + \frac{1}{Re}T_{1l}, \tag{58}$$

$$-\hat{\omega}\hat{a}\Psi_{1l} + \hat{a}^2\Psi_{0lz}\Psi_{1l} = -Dp_{1l} - i\hat{a}\frac{1}{Re}(D^2 - \hat{a}^2)\Psi_{1l}, \tag{59}$$

$$-i\hat{\omega}T_{1l} - i\hat{a}\Psi_{1l}T_{0lz} + i\hat{a}\Psi_{0lz}T_{1lx} = \frac{1}{Pr_l Re}(D^2 - \hat{a}^2)T_{1l}, \tag{60}$$

where  $D = d/dz$ . One can eliminate the pressure perturbation  $p_{1l}$  from Eqs. (58) and (29), and obtain

$$\frac{1}{Re}(D^2 - \hat{a}^2)^2\Psi_{1l} - i\hat{a}\left(\Psi_{0lz} - \frac{\hat{\omega}}{\hat{a}}\right)(D^2 - \hat{a}^2)\Psi_{1l} + i\hat{a}\Psi_{0lzz}\Psi_{1l} + \frac{1}{Re}DT_{1l} = 0.$$

The final set of linear equations reads as follows:

$$\frac{1}{Re}(D^2 - \hat{a}^2)^2\Psi_{1l} - i\hat{a}\left(\Psi_{0lz} - \frac{\hat{\omega}}{\hat{a}}\right)(D^2 - \hat{a}^2)\Psi_{1l} + i\hat{a}\Psi_{0lzz}\Psi_{1l} + \frac{1}{Re}DT_{1l} = 0, \tag{61}$$

$$\frac{v}{Re}(D^2 - \hat{a}^2)^2\Psi_{1v} - i\hat{a}\left(\Psi_{0vz} - \frac{\hat{\omega}}{\hat{a}}\right)(D^2 - \hat{a}^2)\Psi_{1v} + i\hat{a}\Psi_{0vzz}\Psi_{1v} + \frac{1}{Re}\alpha DT_{1v} = 0, \tag{62}$$

$$\frac{1}{Pr_l Re}(D^2 - \hat{a}^2)T_{1l} - i\hat{a}\left(\Psi_{0lz} - \frac{\hat{\omega}}{\hat{a}}\right)T_{1l} + i\hat{a}T_{0lz}\Psi_{1l} = 0, \tag{63}$$

$$\frac{v}{Pr_v Re}(D^2 - \hat{a}^2)T_{1v} - i\hat{a}\left(\Psi_{0vz} - \frac{\hat{\omega}}{\hat{a}}\right)T_{1v} + i\hat{a}T_{0vz}\Psi_{1v} = 0. \tag{64}$$

Let us introduce a new parameter  $x_R$

$$x_R = \left(\frac{x_0}{Re}\right)^{1/4},$$

where  $x_0$  denotes the scaled distance from the leading edge along the vertical wall. The basic-flow stream functions,  $\Psi_{0l}$  and  $\Psi_{0v}$ , may be expressed through the basic-flow functions,  $f_{0l}(\eta)$  and  $f_{0v}(\eta)$ , as follows:

$$\Psi_{0l}(z) = x_R^3 f_{0l}(\eta), \quad \Psi_{0v}(z) = vx_R^3 f_{0v}(\eta).$$

The corresponding quantities for the first-order stream functions are:

$$\Psi_{1l}(z) = x_R^3 f_{1l}(\eta), \quad \Psi_{1v}(z) = vx_R^3 f_{1v}(\eta).$$

The operator  $D_\eta$  (derivative in  $\eta$ ) is expressed as

$$D_\eta = x_R D.$$

We also introduce new wave number and frequency (depending on the position  $x_0$ ) as follows:

$$a = x_R \hat{a}, \quad \omega = \frac{\hat{\omega}}{x_R}.$$

Using these quantities we may rewrite the Eqs. (61) and (63):

$$\frac{1}{\mathcal{R}}(D_\eta^2 - a^2)^2 f_{1l} - ia\left(f'_{0l} - \frac{\omega}{a}\right)(D_\eta^2 - a^2)f_{1l} + ia f'''_{0l} f_{1l} + \frac{1}{\mathcal{R}}g'_{1l} = 0, \tag{65}$$

$$\frac{1}{Pr_l \mathcal{R}}(D_\eta^2 - a^2)g_{1l} - ia\left(f'_{0l} - \frac{\omega}{a}\right)g_{1l} + ia g'_{0l} f_{1l} = 0, \tag{66}$$

where we set  $T_{0l}(z) = g_{0l}(\eta)$ ,  $T_{1l}(z) = g_{1l}(\eta)$ , and define a new parameter  $\mathcal{R}$

$$\mathcal{R} = Re x_R^3.$$

$\mathcal{R}$  is given by

$$\mathcal{R} = Gr^{1/4} x_0^{3/4} = \left(\frac{g\alpha_l \Delta T x_{0d}^3}{\nu_l^2}\right)^{1/4},$$

which depends both on the *dimensional* position  $x_{0d}$  along the wall, and the temperature difference (or evaporation number  $E$ ). The dimensional wavenumber is then

$$a_d = \left(\frac{g\alpha_l \Delta T}{\nu_l^2 x_{0d}}\right)^{1/4} a.$$

The corresponding equations in the vapor are

$$\frac{1}{\mathcal{R}}(D_\eta^2 - a^2)^2 f_{1v} - ia\left(f'_{0v} - \frac{\omega}{va}\right)(D_\eta^2 - a^2)f_{1v} + ia f'''_{0v} f_{1v} + \frac{\alpha}{\nu^2 \mathcal{R}}g'_{1v} = 0, \tag{67}$$

$$\frac{1}{Pr_v \mathcal{R}}(D_\eta^2 - a^2)g_{1v} - ia\left(f'_{0v} - \frac{\omega}{va}\right)g_{1v} + ia g'_{0v} f_{1v} = 0. \tag{68}$$

The set of the interface boundary conditions is

$$T_{11} + h_1 T_{01z} = 0, \tag{69}$$

$$T_{1v} + h_1 T_{0vz} = 0, \tag{70}$$

$$\frac{E}{Re} J_1 + i h_1 \hat{a} \left( \Psi_{01z} - \frac{\hat{\omega}}{\hat{a}} \right) + i \hat{a} \Psi_{11} = 0, \tag{71}$$

$$\rho^{-1} \frac{E}{Re} J_1 + i h_1 \hat{a} \left( \Psi_{0vz} - \frac{\hat{\omega}}{\hat{a}} \right) + i \hat{a} \Psi_{1v} = 0, \tag{72}$$

$$D(\Psi_{11} - \Psi_{1v}) + h_1(\Psi_{01zz} - \Psi_{0vzz}) = 0, \tag{73}$$

$$(D^2 + \hat{a}^2)(\Psi_{11} - \mu \Psi_{1v}) + h_1(\Psi_{01zzz} - \mu \Psi_{0vzzz}) = 0, \tag{74}$$

$$p_{11} - p_{1v} + \frac{2E^2 J_0 J_1}{Re^2} (1 - \rho^{-1}) - \frac{2i\hat{a}}{Re} D(\Psi_{11} - \mu \Psi_{1v}) - \frac{2i\hat{a}}{Re} h_1(\Psi_{01zz} - \mu \Psi_{0vzz}) = -\frac{S}{Re^2} \hat{a}^2 h_1, \tag{75}$$

$$D(T_{11} - kT_{1v}) + h_1(T_{01zz} - kT_{0vzz}) + J_1 = 0. \tag{76}$$

Let us rewrite these conditions using similarity variable with the interface perturbation and the mass flux rescaled by  $h_1 = H_1 x_R$ ,  $J_1 = \bar{J}_1 / x_R$ :

$$g_{11} + H_1 g'_{01} = 0, \tag{77}$$

$$g_{1v} + H_1 g'_{0v} = 0, \tag{78}$$

$$\frac{E}{\mathcal{R}} \bar{J}_1 + i H_1 a \left( f'_{01} - \frac{\omega}{a} \right) + i a f_{11} = 0, \tag{79}$$

$$\mu^{-1} \frac{E}{\mathcal{R}} \bar{J}_1 + i H_1 a \left( f'_{0v} - \frac{\omega}{va} \right) + i a f_{1v} = 0, \tag{80}$$

$$(f'_{11} + H_1 f''_{01}) - v(f'_{1v} + H_1 f''_{0v}) = 0, \tag{81}$$

$$(D_\eta^2 + a^2)(f_{11} - \mu v f_{1v}) + H_1 D_\eta^3(f_{01} - \mu v f_{0v}) = 0, \tag{82}$$

$$P_{11} - P_{1v} + \frac{2E^2 \bar{J}_0 \bar{J}_1}{\mathcal{R}} (1 - \rho^{-1}) - 2ia(f'_{11} - \mu v f'_{1v}) - 2iaH_1(f''_{01} - \mu v f''_{0v}) = -\frac{S}{\mathcal{R}} a^2 H_1, \tag{83}$$

$$(g'_{11} - k g'_{1v}) + H_1(g''_{01} - k g''_{0v}) + \bar{J}_1 = 0 \tag{84}$$

and where rescaled pressure perturbations are used  $p_{11} = x_R Re^{-1} P_{11}$ ,  $p_{1v} = x_R Re^{-1} P_{1v}$ . The rescaled basic-flow mass flux  $\bar{J}_0 = J_0 x_R$  is determined as

$$\bar{J}_0 = -\frac{3E}{4\mathcal{R}} f_{01}(\bar{\eta}) = -\frac{3E}{4\mathcal{R}\mu} f_{0v}(\bar{\eta}).$$

Rescaled equation (58) and a similar one for the vapor phase could be used for determination of pressure perturbations.

$$\begin{aligned} & -ia \left( \frac{\omega}{a} f'_{11} + f''_{01} f_{11} - f'_{01} f'_{11} \right) \\ & = \frac{1}{\mathcal{R}} (-ia P_{11} + (D_\eta^2 - a^2) D_\eta f_{11} + g_{11}), \\ & -ia \left( \frac{\omega}{va} f'_{1v} + f''_{0v} f_{1v} - f'_{0v} f'_{1v} \right) \\ & = \frac{1}{\mathcal{R}} \left( -\frac{ia}{\mu v} P_{1v} + (D_\eta^2 - a^2) D_\eta f_{1v} + \frac{\alpha}{v^2} g_{1v} \right). \end{aligned}$$

One can now determine the stability properties of the basic state for quasi-parallel, two-dimensional disturbances.

## 7. Numerical results and discussion

### 7.1. Numerical procedure

The linear stability problem is solved as a spatial-growth problem, i.e. the wave number  $a$  is assumed to be complex,  $a = a_R + ia_I$  with real time frequency  $\omega$  of the perturbation. For fixed parameters of the problem and selected  $\omega$  we determine the complex eigenvalue of the wave number  $a$ ; the positive  $a_I$  corresponds to decay of disturbances, while negative  $a_I$  means that the disturbance grows in the direction of the flow along the wall. Hence, the neutral curve is given by the condition  $a_I = 0$ . Satisfaction of the boundary conditions for the liquid phase requiring that all first-order quantities vanish exponentially far from the wall is attained using the method discussed in [7]. The results of calculations are checked against that of a standard temporal-stability analysis with complex  $\omega$  and real  $a$  using the Gaster theorem [10]. Once the most unstable branch is detected we use a continuation technique in order to follow this branch. The eigenvalue problem in three-dimensional complex space is solved by the gradient method using the hybrid symbolic-numeric code written in *Mathematica* computer algebra language.

### 7.2. Neutral curves for one-phase problem

The linear-stability calculations are performed for the one-phase problem for air, water and ethanol, and the resulting neutral curves are shown in Fig. 3. In case of air both shear and thermal instabilities are found represented by lower and upper lobes of the curve, respectively. For water and ethanol only one lobe is found, indicating that both instabilities overlap in these cases. These results are in good agreement with those of Nachtshiem [7]. The positions of critical points of the neutral curves are  $\mathcal{R}_c = 16.9$ ,  $a_c = 0.154$  for water,  $\mathcal{R}_c = 22.2$ ,  $a_c = 0.122$  for air, and  $\mathcal{R}_c = 12.1$ ,  $a_c = 0.246$  for ethanol.



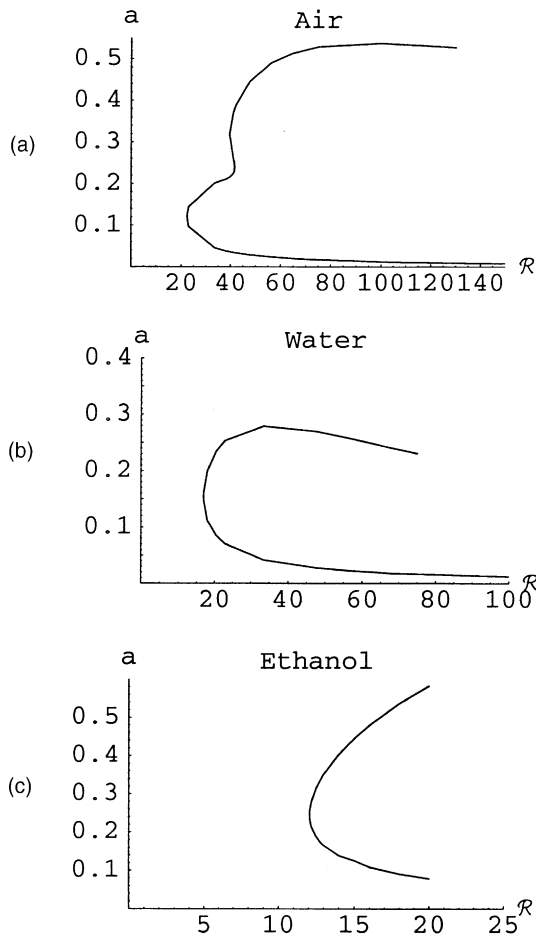


Fig. 3. The neutral curves in the one-phase case for (a) air, (b) water, and (c) ethanol.

7.3. Neutral curves for the two-phase problem for water (with surface tension set to zero)

The dependence of the neutral curve profile is determined on two dimensionless temperature parameters, the overall temperature difference (or evaporation number  $E$ ) and the relative superheat  $A$  which controls the thickness of the vapor film. In the range  $0.01 \leq E \leq 10.0$  no significant influence is found of this parameter on the neutral curve (when it is depicted in  $\{R, a\}$  plane). In Fig. 4 the neutral curves are presented for water with its vapor at different values of overall superheat given by the evaporation number  $E$  and fixed relative superheat  $A = 0.2$ .

The relative superheat  $A$  strongly affects the upper branch of the neutral curve and has very weak influences on the lower branch and the most dangerous value  $R_c$ , as shown in Fig. 5 ( $A = 0.2 : R_c = 20.0, a_c = 0.145, A = 0.5 : R_c = 24.2, a_c = 0.108, A = 0.8 : R_c = 23.1,$

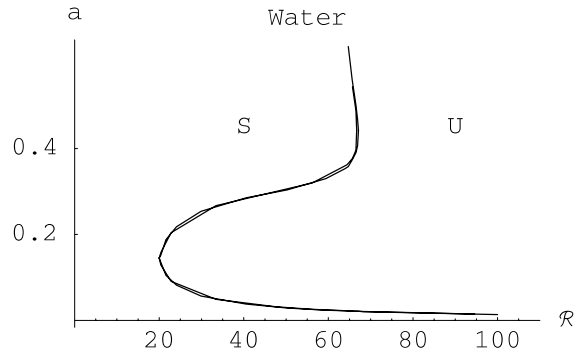


Fig. 4. The neutral curves for water for  $A = 0.2$  and  $0.01 \leq E \leq 10.0$  ( $10 \leq \Delta T \leq 10^4$  °C).

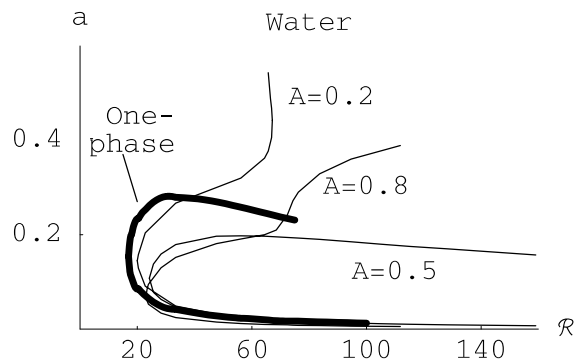


Fig. 5. The neutral curves for water for  $E = 0.1$  ( $\Delta T = 100$  °C) and different thicknesses of the vapor film in two-phase problem and for one-phase problem (thick curve).

$a_c = 0.072$ ). The location of the upper branch of the neutral curve is not monotonic with the increase of  $A$ , though, as shown in Fig. 5 the one-phase  $R_c$  and  $a_c$  are approached as  $A \rightarrow 0$ .

7.4. Neutral curves for the two-phase problem for ethanol (with surface tension set to zero)

Results of the linear stability analysis for ethanol show that in this case there is a noticeable influence of the evaporation number on the critical value of Reynolds number  $R_c$ , while the most dangerous wave number is not affected, as shown in Fig. 6 ( $E = 0.01 : R_c = 16.90, a_c = 0.125, E = 0.1 : R_c = 18.29, a_c = 0.122, E = 1.0 : R_c = 18.44, a_c = 0.121$ ).

Fixing the evaporation number  $E$  enables us to check the influence of the relative superheat on the two-phase flow stability characteristics for ethanol, as shown in Fig. 7. It appears that small  $A$  (thin vapor film) corresponds to smaller critical values of  $R_c$ , larger critical

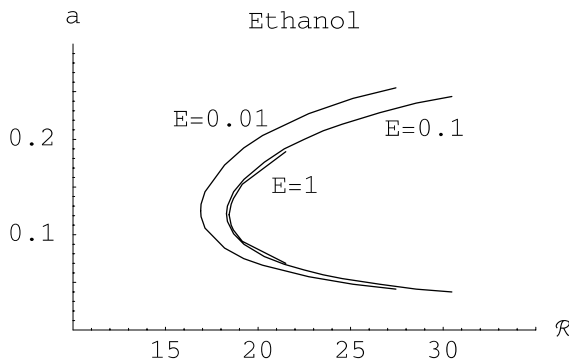


Fig. 6. The neutral curves for ethanol for  $A = 0.8$  and  $0.01 \leq E \leq 1.0$  ( $18 \leq \Delta T \leq 1830$  °C).

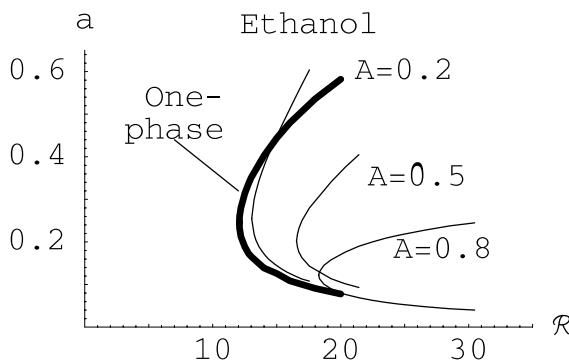


Fig. 7. The neutral curves for ethanol for  $E = 0.1$  ( $\Delta T = 183$  °C) and different thicknesses of the vapor film in two-phase problem and for one-phase problem (thick curve).

wave numbers and wider instability zone ( $A = 0.2$ :  $\mathcal{R}_c = 13.04$ ,  $a_c = 0.255$ ,  $A = 0.5$ :  $\mathcal{R}_c = 16.55$ ,  $a_c = 0.203$ ,  $A = 0.8$ :  $\mathcal{R}_c = 18.29$ ,  $a_c = 0.122$ ). Notice in Fig. 7 that the one-phase  $\mathcal{R}_c$  and  $a_c$  are approached as  $A \rightarrow 0$ .

#### 7.5. Approximate neutral curves for the two-phase problem for water (with non-zero surface tension)

In the above analysis the surface tension parameter  $S$  was taken to be zero, consistent with the self-similar basic state examined. One would like to estimate the effect of reasonably small surface tension on the neutral curves. To this end, consider a *model* system in which  $S = 0$  in the basic state, but  $S > 0$  in the disturbance equations.

The results of calculations show that as  $S$  increases from zero, the flow becomes more stable, especially for large wave numbers. Fig. 8 shows such neutral curves for  $A = 0.2$ ,  $E = 0.1$  and for  $S = 0$  and  $S = 10^6$ . As  $S \rightarrow \infty$ , the basic state in this model becomes unconditionally stable; all infinitesimal perturbations decay, as

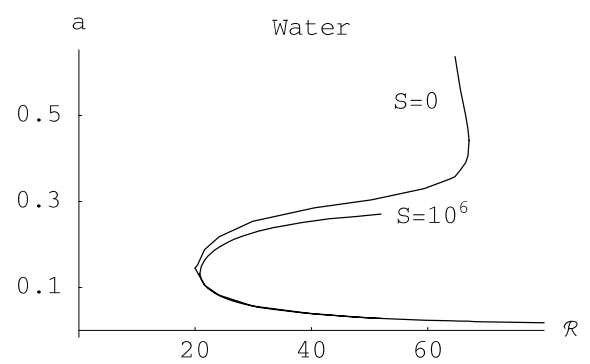


Fig. 8. The neutral curves for water for  $A = 0.2$ ,  $E = 0.1$  and with changing dimensionless surface tension  $S$  ( $S = 0$ :  $\mathcal{R}_c = 20.05$ ,  $a_c = 0.145$ ,  $S = 10^6$ :  $\mathcal{R}_c = 21.7$ ,  $a_c = 0.134$ ).

can be shown analytically (of course,  $S \rightarrow \infty$  is the least likely limit that this model has physical significance). Thus, for reasonable values of parameters the critical wave numbers are small enough, so that the influence of surface tension is small, indicating that the instabilities that emerge are driven by the bulk fields, and not by the interface.

#### 7.6. Discussion

Fig. 2 shows that the temperature and velocity profiles for the two-phase problem are markedly similar to those of the one-phase case, suggesting that the neutral curves in the two cases may be similar as well. This is borne out in the comparisons between Figs. 3 and 5. Here in Fig. 3(a) for air there is a two-lobe structure reminiscent of that in Fig. 5 for  $A = 0.2$ , for example. Fig. 3(b) for water has only a single lobe similar to that of in Fig. 5 for  $A = 0.5$ . It is clearly seen that the critical point of the neutral curve for two-phase problem approaches similar point for one-phase case when  $A$  (and the thickness of the vapor film) decreases reaching zero.

The evaporation number  $E$  has little influence on the neutral curves in typical operating ranges. However, the superheat  $A$ , which controls the thickness of the vapor film, affects the stability conditions significantly. Fig. 7 shows that in the range  $A \in [0.2, 0.8]$ ,  $\mathcal{R}_c \in [13]$  and  $a_c \in [0.10, 0.25]$ .

In all cases the self-similar basic state suggests that the instability parameters depend on  $x_{0d}$ , the distance from the leading edge. Here,

$$\mathcal{R} = \left( \frac{g\alpha_1 \Delta T x_{0d}^3}{v_1^2} \right)^{1/4}, \quad a = \left( \frac{v_1^2 x_{0d}}{g\alpha_1 \Delta T} \right)^{1/4} a_d,$$

where  $a_d$  is the dimensional wave number.

For the chosen sample materials we therefore may predict the dimensional critical distance  $(x_{0d})_c$  from the leading edge for various superheat values:

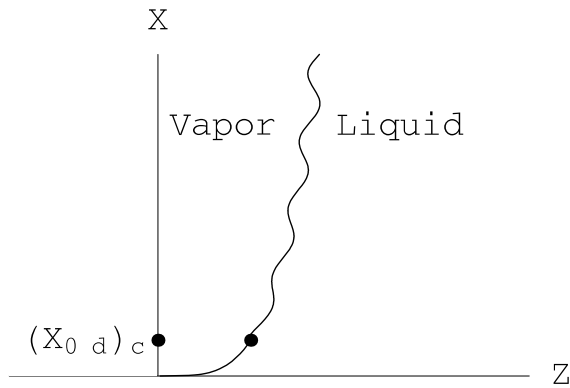


Fig. 9. The typical snapshot of the vapor–liquid interface for water for  $A = 0.5$ ,  $E = 0.1$ . Growth of disturbances begins at  $x = (x_{0d})_c$ .

	Water	Ethanol
$A$	$(x_{0d})_c$ (m)	$(x_{0d})_c$ (m)
0.2	$0.62 \times 10^{-3}$	$0.44 \times 10^{-3}$
0.5	$0.80 \times 10^{-3}$	$0.60 \times 10^{-3}$
0.8	$0.75 \times 10^{-3}$	$0.69 \times 10^{-3}$

Below this critical point all perturbations decrease, and beyond it they start to grow in space. As the result the typical instantaneous snapshot of the vapor–liquid interface at neutral stability will have a form shown in Fig. 9.

We chose the method of spatial stability analysis in which the perturbation has a fixed time frequency and we followed its spatial-growth rate along the wall in the direction of the flow. The main assumption usually made in such computations is the quasi-parallel approximation when all  $x$  derivatives (along the wall) of the basic-flow quantities are set to be zero. This assumption corresponds to local rather than global stability characteristics. Some authors (see, for example, [11]) suggest a method of “globalization” or averaging of the local characteristics. The idea is to integrate the locally determined spatial-growth rate starting from the point of instability onset to some arbitrary position along the wall. We have calculated the averaged neutral curve for  $A = 0.2$ ,  $E = 0.1$ , and the comparison shows (see Fig. 10) that while the local curve represents two instabilities, the averaged curve shows only one instability, and it has a narrower instability range in wave numbers (or time frequencies).

The linear stability analysis of two-phase (and even one-phase) problems is a challenge from computational point of view. It was noted already in [7] that the calculations for larger values of wave numbers (or time frequencies) demonstrated rapid deterioration in accuracy which cannot be cured by known approaches. We were able to improve some results for one-phase models

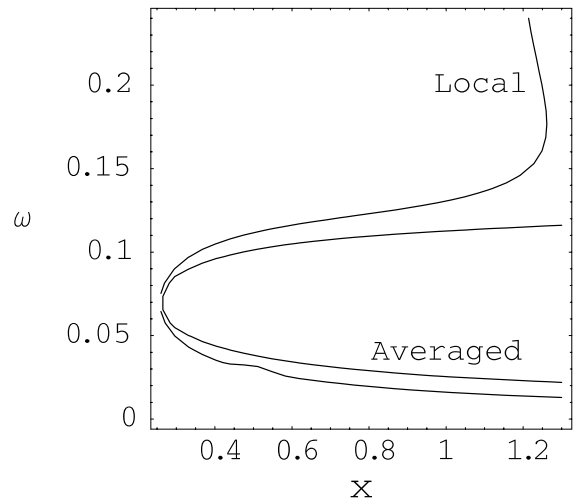


Fig. 10. The comparison of local and averaged neutral curves for  $A = 0.2$ ,  $E = 0.1$ .

(see Fig. 3), but we found the same type of numerical instabilities in the two-phase problem.

In scaling the equations, velocity scale (29) was chosen meaning that Reynolds number equals to the Grashof number. Instead, one could choose other scalings corresponding to a general relation  $Gr = Re^{2-\beta}$ . In the case the basic flow is still self-similar, and in terms of scaled variables its stability criteria remain unchanged for  $\beta < 3/2$ , i.e. as long as mass flux  $J$  neglected in (45).

### Acknowledgements

This work was supported by a grant DE-FG02-86ER13641 of the Engineering Research Program of the Office of Basic Energy Sciences at the Department of Energy.

### References

- [1] D.H. Sharp, An overview of Rayleigh–Taylor instability, *Physica D* 12 (1984) 3–18.
- [2] H.K. Fauske, Some aspects of liquid–liquid heat transfer and explosive boiling, in: *Proc. of Fast Reactor Safety Meeting*, Beverly Hills, California, 1974, p. 992.
- [3] S.G. Bankoff, H.K. Fauske, On mechanisms of vapor explosions, *Nucl. Sci. Eng.* 54 (1974) 481–482.
- [4] K.L. Waldram, H.K. Fauske, S.G. Bankoff, Impact of volatile liquid drops onto a hot liquid surface, *Can. J. Chem. Eng.* 54 (1976) 456–481.
- [5] V.P. Skripov, *Metastable Liquids*, John Wiley and Sons, New York, 1974, 272 pp.
- [6] K. Hata, K. Fukuda, M. Shiotsu, A. Sakurai, The effect of diameter on critical heat flux in vertical heated short tubes

- of various inside diameters cooled with an upward flow of subcooled water, in: Ninth International Topical Meeting on Nuclear Reactor Thermal Hydraulics (NURETH-9), San Francisco, California, October 3–8, 1999, 35 pp.
- [7] P.R. Nachtshiem, Stability of free-convection boundary layer flows, NASA Technical Notes D-2089, 1963.
- [8] B. Gebhart, Natural convection flow, instability, and transition, *J. Heat Transfer* 91 (1969) 293–309.
- [9] J.P. Burelbach, S.G. Bankoff, S.H. Davis, Nonlinear stability of evaporating/condensing liquid films, *JFM* 195 (1988) 463–494.
- [10] M. Gaster, A note on the relation between temporally-increasing and spatially-increasing disturbances in hydrodynamic stability, *J. Fluid Mech.* 14 (1962) 222–224.
- [11] T. Herbert, Parabolized stability equation, *Annu. Rev. Fluid Mech.* 29 (1997) 245–283.